Oncogene (2011) 30, 4498–4508

www.nature.com/onc

Open

ORIGINAL ARTICLE

IRX1 influences peritoneal spreading and metastasis via inhibiting BDKRB2-dependent neovascularization on gastric cancer

J Jiang[1], W Liu[1], X Guo, R Zhang, Q Zhi, J Ji, J Zhang, X Chen, J Li, J Zhang, Q Gu, B Liu, Z Zhu and Y Yu

Department of Surgery, Shanghai Ruijin Hospital and Shanghai Institute of Digestive Surgery, Shanghai Key Laboratory of Diagnosis and Treatment for Gastric Cancer, Shanghai Jiao Tong University, School of Medicine, Shanghai, China

The overexpression of *IRX1* gene correlates with the growth arrest in gastric cancer. Furthermore, overexpression of *IRX1* gene suppresses peritoneal spreading and long distance metastasis. To explore the precise mechanisms, we investigated whether restoring IRX1 expression affects the angiogenesis or vasculogenic mimicry (VM). Human umbilical vein endothelial cells (HUVECs) and chick embryo and SGC-7901 gastric cancer cells were used for angiogenesis and VM analysis. Small interfering RNA was used for analyzing the function of BDKRB2, a downstream target gene of IRX1. As results, the remarkable suppression on peritoneal spreading and pulmonary metastasis of SGC-7901 cells by *IRX1* transfectant correlates to reduced angiogenesis as well as VM formation. Using the supernatant from SGC-7901/*IRX1* cells, we found a strong inhibiting effect on angiogenesis both *in vitro* and in chick embryo. SGC-7901/*IRX1* cells revealed strong inhibiting effect on VM formation too. By gene-specific RNA interference for BDKRB2, or its effector PAK1, we got an effective inhibition on tube formation, cell proliferation, cell migration and invasion *in vitro*. In conclusion, enforcing IRX1 expression effectively suppresses peritoneal spreading and pulmonary metastasis via anti-angiogenesis and anti-VM mechanisms, in addition to previously found cell growth and invasion. BDKRB2 and its downstream effector might be potential targets for anti-cancer strategy.

Oncogene (2011) **30,** 4498–4508; doi:10.1038/onc.2011.154; published online 23 May 2011

Keywords: gastric carcinoma; IRX1; angiogenesis; vasculogenic mimicry; BDKRB2

Introduction

IRX1 is a newly identified tumor suppressor gene on gastric cancer in our previous studies (Lu *et al*., 2005; Guo *et al*., 2010). Meanwhile, the tumor suppressor function of *IRX1* was also confirmed on head and neck squamous cell carcinoma by others (Bennett *et al*., 2008, 2009). *IRX1* belongs to Iroquois homeobox gene family, which has six members of *IRX1* to *IRX6*. *IRX1* is closely related to embryonic development, including foregut organs such as lung (Becker *et al*., 2001; Alarcon *et al*., 2008). Our previous study revealed that restoring IRX1 in gastric cancer cells arrested cancer proliferation both *in vitro* and *in vivo*. In addition, we found that several downregulated genes involve in angiogenesis in *IRX1*-transfected gastric cancer cells by cDNA microarray analysis (GSE17399). *BDKRB2* is one of the downregulated genes, which connects to angiogenesis in several tumors (Ishihara *et al*., 2002; Wu *et al*., 2002). Growth of solid tumor relies on blood vessels to supply oxygen and nutrients. Tumor progression is accompanied by flourish neovascularization to satisfy its metabolic demands. Endothelium-dependent vessels are the predominant microcirculatory mechanism for solid tumors. Therefore, endothelium is the target of the anti-angiogenesis treatment (Matsuda *et al*., 2000; Getmanova *et al*., 2006). Vasculogenic mimicry (VM) of solid tumor is another microcirculatory mechanism, which is an endothelium-independent pattern. Various types of malignant tumors demonstrated internal blood supply network via VM formation, including malignant melanoma (Maniotis *et al*., 1999), inflammatory breast cancer (Shirakawa *et al*., 2003) prostate cancer (Sharma *et al*., 2002), invasive ovarian cancer (Su *et al*., 2008), sarcoma (Hao *et al*., 2002), astrocytoma (Yue and Chen, 2005) and so on. VM is strongly associated with a poor prognosis in human tumors. So, VM becomes a potential target for anti-cancer strategy (Fujimoto *et al*., 2006; Zhang *et al*., 2007; Sun *et al*., 2008).

Gastric cancer is one of the common solid malignancies characterized by accumulated genetic and epigenetic alterations. Peritoneal spreading and metastasis are the pivotal factors for its poor prognosis. Many efforts have been made to arrest the peritoneal spreading and long distance metastasis for gastric cancer. In this paper, we report a new finding that enforcing *IRX1* expression disclosed anti-spreading and anti-metastasis efficacies in

Correspondence: Dr Y Yu or Dr Z Zhu, Department of Surgery, Ruijin Hospital and Shanghai Institute of Digestive Surgery, ShanghaiJiao Tong University, School of Medicine, Ruijin er Road, No. 197, Shanghai 200025, PR China.
E-mail: yingyan3y@yahoo.com.cn or surgeryzhu@yahoo.com.cn
[1]These authors contributed equally to this work.
Received 10 October 2010; revised 26 March 2011; accepted 27 March 2011; published online 23 May 2011

animal experiments. The biological functions closely depend on the activity of *BDKRB2* gene. *BDKRB2* (bradykinin receptor B2, NM-000623.3) is also termed B2R or BK-2 receptor. This gene encodes a receptor for bradykinin, which elicits many responses including vasodilation, edema, smooth muscle spasm and pain fiber stimulation. Some study revealed that bradykinin regulates the secretion and biosynthesis of endothelin-1 through kinin B2 receptor in melanoma cells (Andoh *et al*., 2010). Although BDKRB2 expression has been identified on some cancer tissues (Wu *et al*., 2002), little is known about its biological functions on gastric carcinoma, especially on IRX1-related anti-angiogenic mechanism. Our new findings will facilitate the understanding of IRX1-mediated anti-cancer mechanisms on gastric cancer.

Results

Enforcing IRX1 on gastric cancer cells suppresses peritoneal spreading and lung metastasis in nude mice

A total of 75 nude mice were enrolled in these experiments. Among them, 30 mice were used for peritoneal spreading study and 45 for pulmonary metastatic study. The experimental results were summarized in Table 1. The peritoneal nodules were markedly suppressed in IRX1 overexpression group, compared with mock or controls (1.0 ± 0.70 vs 4.4 ± 1.14, $P < 0.001$; Figure 1a). The tumorigenicity of pulmonary metastasis was also observed. In IRX1 overexpression group, 2 out of 15 mice show tumorigenicity in lung, which is significantly lower than that in mock (11/15) and controls (10/15) ($P = 0.002$; Figure 1b). Meanwhile, we assayed the microvessel density by CD34 immunohistochemical stain as well as VM density by periodic acid-schiff (PAS) histochemical stain. We found a significant reduction of microvessel density and VM density in tumor tissues of SCG-7901/*IRX1* group, compared with mock or controls (Figure 2).

Enforcing IRX1 on gastric cancer cells suppresses tubular formation of HUVECs

Human umbilical vein endothelial cells (HUVECs) (2×10^4 cells/well) were suspended in collected supernatants from SGC-7901, SGC-7901/vector and SCG-7901/*IRX1*, respectively. After 18 h incubation at 37 °C

Table 1 Animal experiments for peritoneal spreading and pulmonary metastasis

Animal models	*Cells lines*	*Cell number*	*Time*	*Tumorigenicity*	P-*value*
Peritoneal spreading	SGC-7901	2×10^6	4 weeks	4.4 ± 1.14	
	SGC-7901/vector	2×10^6	4 weeks	4.2 ± 0.83	<0.001
	SGC-7901/*IRX1*	2×10^6	4 weeks	1.0 ± 0.70	
Pulmonary metastasis	SGC-7901	2×10^6	2 months	11/15	
	SGC-7901/vector	2×10^6	2 months	10/15	0.002
	SGC-7901/*IRX1*	2×10^6	2 months	2/15	

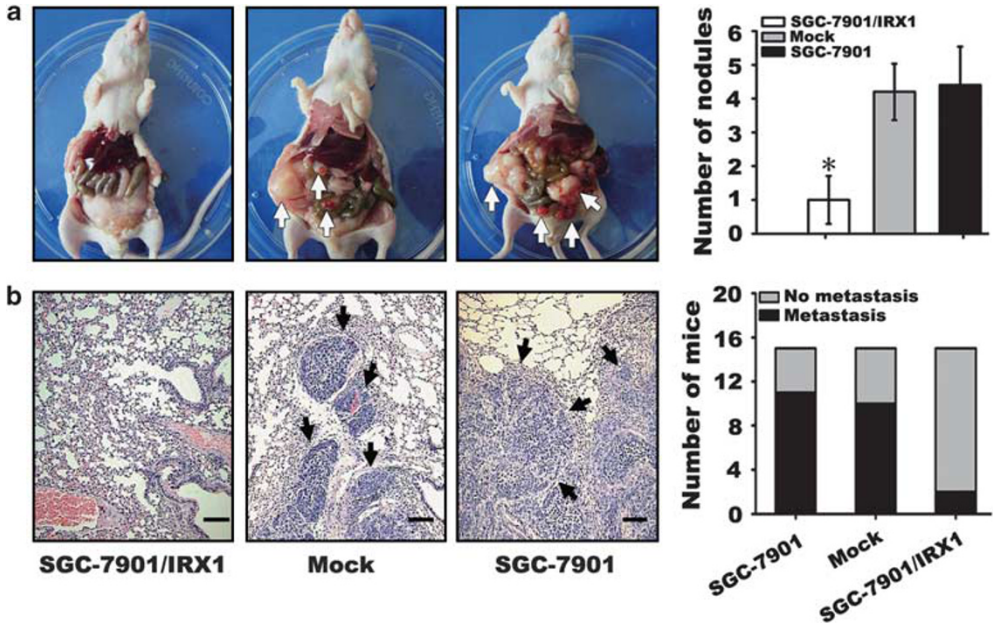

Figure 1 Effect of enforcing IRX1 on peritoneal spreading and metastasis. A 0.1-ml suspension (2×10^6 cells/ml) per mouse was injected into peritoneal cavity or caudal vena. (**a**) The peritoneal nodules were markedly suppressed in IRX1 overexpression group, compared with mock or controls (1.0 ± 0.70 vs 4.2 ± 0.83, 4.4 ± 1.14, $^*P < 0.001$). (**b**) Metastatic cancer mass is easily observed microscopically in mock or controls, compared with experimental animal (the tumor is indicated with arrow, the bar indicates 50 μm). In IRX1 overexpression group, 2 out of 15 mice show tumorigenicity in lung, which is significantly lower than that in mock (11/15) and controls (10/15) ($P = 0.002$).

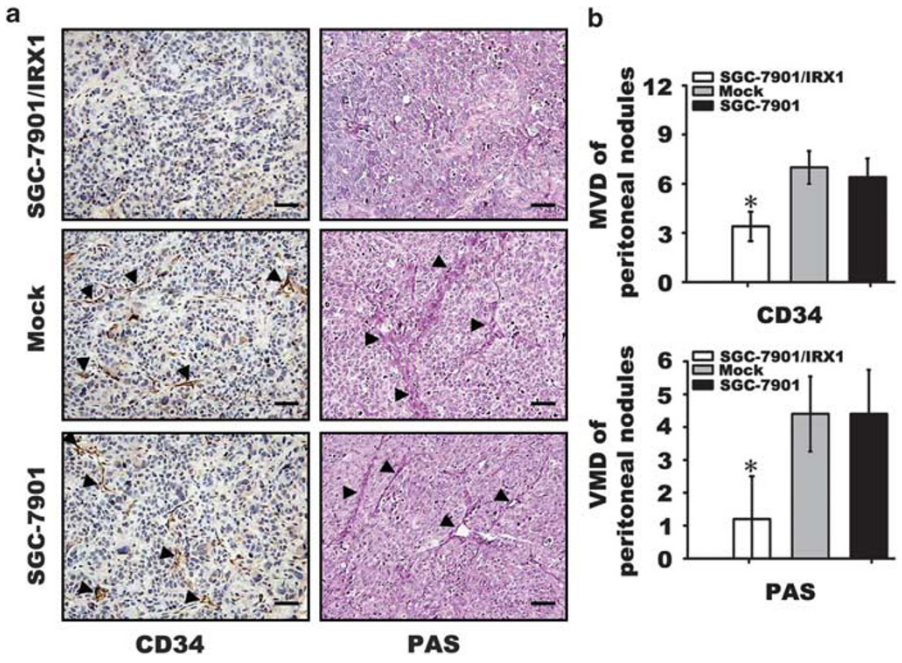

Figure 2 Assays of microvessel density (MVD) or vasculogenic mimicry density (VMD) on tumor tissues. (**a**) MVD of tumor tissues was assayed by CD34 immunohistochemistry. A significant reduction of MVD in tumor tissues of SCG-7901/*IRX1* group, compared with mock or controls (3.8 ± 0.83 vs 7.4 ± 1.51 or 6.8 ± 1.30, $^*P < 0.001$, the bar indicates 20 μm). (**b**) VMD of tumor tissues was assayed by PAS histochemistry. A significant reduction of VMD in tumor tissues of SCG-7901/*IRX1* group, compared with mock or controls (1.20 ± 1.30 vs 4.4 ± 1.14 or 4.4 ± 1.34, $^*P = 0.002$, the bar indicates 20 μm).

with 5% CO_2, tubular numbers of each group were assessed under light microscope. The supernatant from SGC-7901/*IRX1* revealed strong inhibiting effect on tubular formation of HUVECs whatever in tubular number, tubular length and tubular intersecting nods, compared with mock or control (Figure 3). To examine the reproducibility of the finding, we assayed tubular formation after IRX1 overexpression on NCI-N87 gastric cancer cells. We got a similar result as described in SGC-7901 cancer cells. The result is presented in Supplementary Figure 1.

Enforcing IRX1 on gastric cancer cells suppresses VM

Plating 1.5×10^5 cells of SGC-7901, SGC-7901/vector and SCG-7901/*IRX1* on the 3D gel, after 4-day culture without changing culture media, the cells were fixed with 4% formaldehyde in phosphate-buffered saline (PBS) for 10 min and stained with PAS. The formation of VM was assessed as PAS-positive extracellular matrix (ECM) surrounded by cancer cells. SGC-7901/*IRX1* cells revealed strong inhibiting effect on VM formation whatever in tubular length and tubular intersecting nods, compared with mock or controls (Figure 4).

Enforcing IRX1 on gastric cancer cells suppresses angiogenesis in chick embryo

A traditional chick embryo chorioallantoic membrane (CAM) assay was used for observing the effect of restoring *IRX1* on angiogenesis. A 30-μl supernatant from SGC-7901, SGC-7901/vector and SCG-7901/*IRX1* was dropped to the surface of the CAM daily, which covered a piece of sterilized filter paper disc. After 3-day treatment, the eggs were photographed, and the vessel numbers around the filter paper disc were assessed. The blood vessel numbers treated with SCG-7901/*IRX1* supernatant were significantly reduced, compared with mock or controls (6.41 ± 2.59 vs 9.18 ± 1.99 and 10.27 ± 2.64, $P = 0.001$; Figure 5).

Enforcing IRX1 on gastric cancer cells suppresses cell-ECM adhesive ability

A 150-μl cell suspension of SGC-7901 (1.0×10^6/ml) was added to the wells coated with fibronectin or collagen IV and incubated for 60 min. After cell staining and washing, we examined the attached cells in the microtiter plate. The OD (optical density) value at 560 nm represents the cell-ECM adhesive ability. The OD 560 value of SGC-7901/*IRX1* cells was significant lower than that in mock or controls on type IV collagen assay (0.576 ± 0.043 vs 0.653 ± 0.059, 0.717 ± 0.061, $P = 0.002$). The OD 560 value of SGC-7901/*IRX1* cells was significant lower than that in mock or controls on fibronectin assays too (0.682 ± 0.040 vs 0.813 ± 0.005, 0.870 ± 0.040, $P < 0.001$).

IRX1 can downregulate BDKRB2 or its downstream effector PAK and influence multiple biological behaviors

Our previous cDNA microarray and chromatin immunoprecipitation implied that BDKRB2 functions as one of downstream targets of IRX1 transcription factor. We transfected *IRX1* to SGC-7901 cancer cells and found that BDKRB2 expressing level was significantly decreased by RT–PCR and western blot (Figure 6a). We knocked down BDKRB2 by gene-specific small

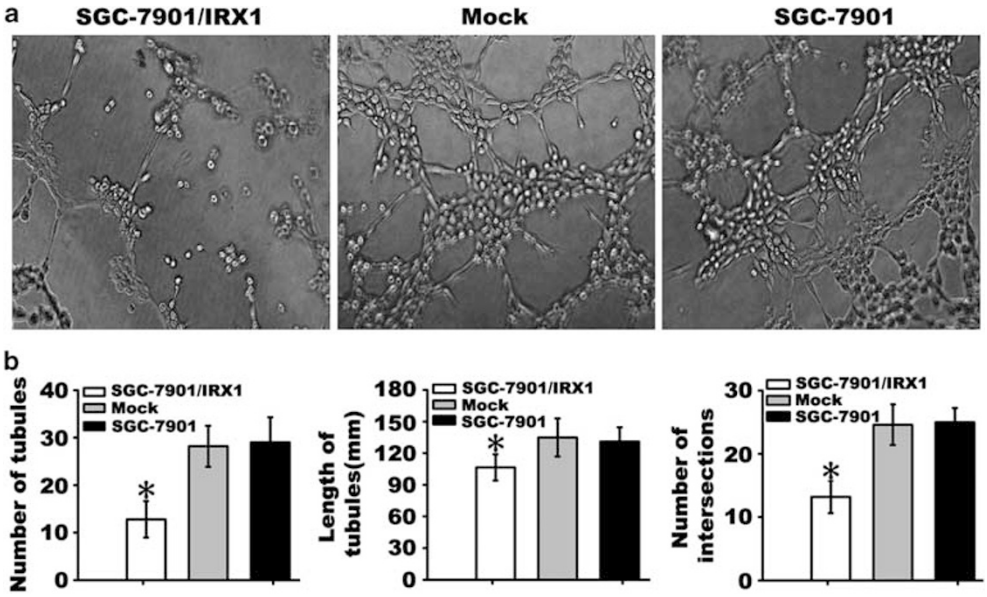

Figure 3 Effect of enforcing *IRX1* on tubular formation *in vitro*. The supernatants from cells with or without *IRX1* transfection were collected. After 18 h co-cultivation with HUVECs, tubular formation was evaluated. (**a**) Poorly formed tubular structure was observed in SCG-7901/*IRX1* group, compared with mock or controls. (**b**) The bar charts represent the counting of tubules number (left, $*P<0.001$), tubular length (middle, $*P=0.022$) and intersecting nods (right, $*P<0.001$) between different groups. The data represent the mean ± s.d. of three independent experiments.

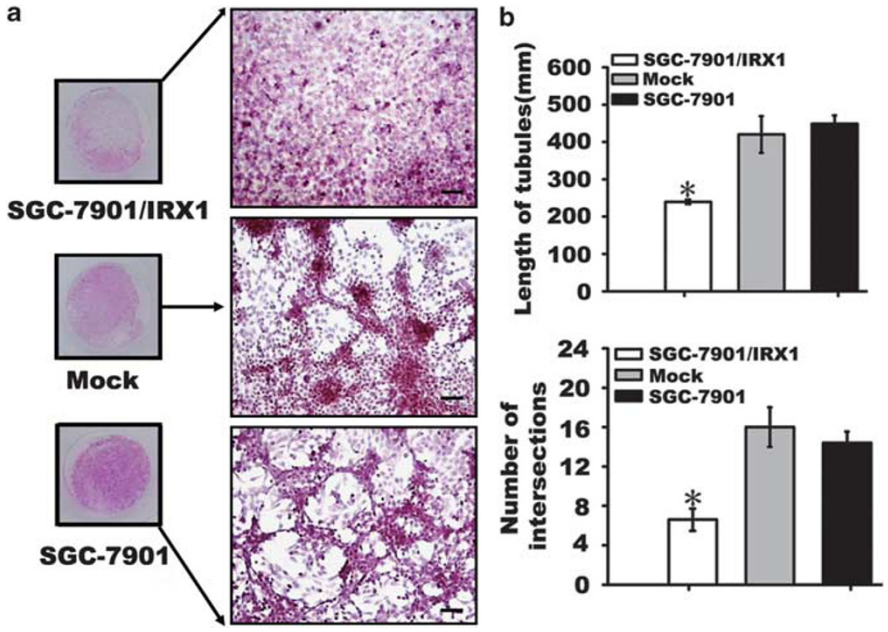

Figure 4 Effect of enforcing *IRX1* on vasculogenic mimicry *in vitro*. Tumor cells of 1.5×10^5 with or without *IRX1* transfection were plated onto the 3D gel plate. After 4-day culture, the cells were stained with PAS reagent. (**a**) Microscopically, less tubular structures with PAS stain were observed in *IRX1* transfectant, compared with mock or controls (the bar indicates 20 μm). (**b**) *IRX1* transfectants revealed strong inhibiting effect on tubular length of vasculogenic mimicry (top, 239.52 μm ± 6.32 vs 419.77 μm ± 48.90 or 448.79 μm ± 22.30, $*P<0.001$) and tubular intersecting nods (down, 6.6 ± 1.14 vs 16 ± 2.0 or 14.4 ± 1.14, $*P<0.001$). Each experiment was performed at least three times.

interfering RNA (siRNA) in SGC-7901 cancer cells, and observed the efficacy on angiogenesis by endothelial tube formation assay. After 48 h siRNA interference, a significant reduction of endothelial tube formation was identified in BDKRB2-siRNA group (11.75 ± 2.36), compared with mock (17.75 ± 1.25) or controls (19.75 ± 2.22), by calculation of the tubular numbers ($P=0.001$; Figure 6b). We introduced siRNA-specific targeting *IRX1* to SGC-7901 cancer cells and found that knockdown of IRX1 in gastric cells reversed the

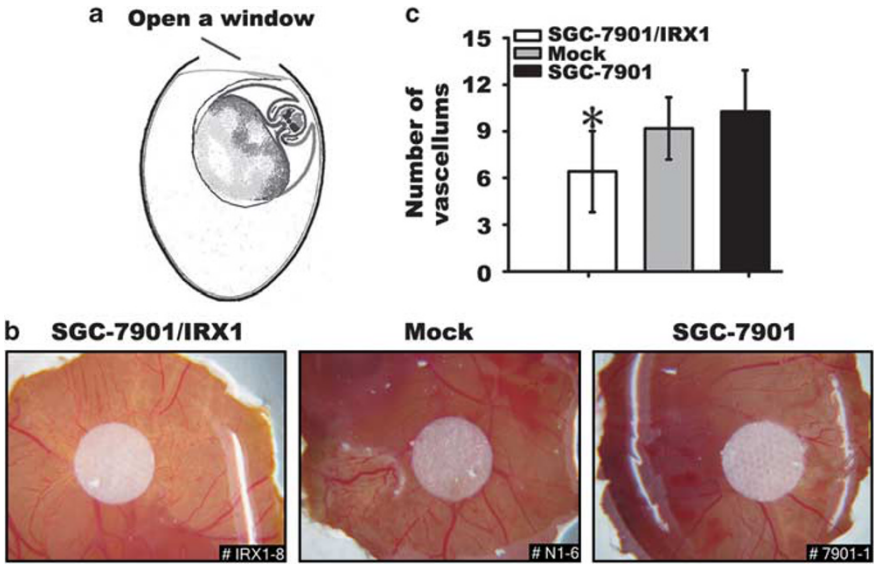

Figure 5 Effect of enforcing *IRX1* on angiogenesis in chick embryo CAM. (**a**) Schematic feature of how to open a window on fertilized chicken egg. (**b**) Dissecting microscope graphs of chick embryos. A remarkable reduction of blood vessels was observed in *IRX1* transfectant, compared with mock or controls. (**c**) The bar chart of vessel numbers around filter. The blood vessel numbers in SCG-7901/*IRX1* (6.41 ± 2.59) group were significantly reduced, compared with mock (9.18 ± 1.99) or control (10.27 ± 2.64, $*P<0.001$).

expression of BDKRB2 significantly (Figure 6c). Meanwhile, we assayed the protein expression of BDKRB2 and IRX1 on peritoneal tumor tissues from nude mice by immunohistochemical stain. We found a significant reduction of BDKRB2 expression in tumor tissues at IRX1 overexpressing group, compared with control (Figure 6d). In wound healing assay, overexpression of IRX1 alone suppressed the cell migration significantly (Figure 6e, lane 2) and overexpression of BDKRB2 alone significantly enhanced the cell migration (Figure 6e, lane 3). Co-expression of BDKRB2 and IRX1 revealed the effect observed as in control (Figure 6e, lane 4). The similar effects on cell migration and invasion were also observed by transwell assay (Figure 6f), along with the cell viability examination. The cell viability in SGC-7901, SCG-7901/*IRX1*, SGC-7901/*BDKRB2* and SGC-7901/*IRX1*/*BDKRB2* at initial point was 97.475 ± 0.502, 97.235 ± 0.728, 96.08 ± 0.438 and 96.065 ± 0.120, respectively ($P=0.09$). The cell viability of above different groups in 24 h point was 93.765 ± 0.771, 91.88 ± 3.295, 93.595 ± 0.813 and 92.15 ± 1.753, respectively ($P=0.71$), and in 48 h point was 84.465 ± 0.134, 81.655 ± 1.746, 83.515 ± 1.972 and 82.75 ± 0.296, respectively ($P=0.32$). To examine the reproducibility of the finding, we compared the wound healing ability after BDKRB2 and IRX1 overexpression on NCI-N87 gastric cancer cells. We got the similar result as described in SGC-7901 cancer cells. The result is presented in Supplementary Figure 1.

By KEGG pathway analysis, p21-activated kinase (PAK) is identified as a key effector in bradykinin pathway. To validate the association of IRX1 and BDKRB2 pathway, we transfected *IRX1*, siRNA-*PAK1* or both *IRX1* and siRNA-*PAK1* to SGC-7901 cells, respectively. We found that overexpression of *IRX1* downregulated PAK1 expressing level, whereas knockdown of *PAK1* level did not alter the IRX1 level significantly (Figure 7a). We examined the cell proliferating activity after *IRX1* overexpression or interfering *PAK1* by siRNA. We found that the cell proliferation was obviously downregulated in *IRX1* overexpressing group or *PAK1* interfering group, compared with controls. Whereas the cell proliferation activity in 7901/*IRX1*/siRNA-*PAK1* group was nearly the same as that observed in *IRX1*-overexpressed cells (Figure 7b). By transwell assays, overexpression of *IRX1* or knockdown of *PAK1* downregulated the transferred cell numbers. Whereas, in 7901/*IRX1*/siRNA-*PAK1* group, the transferred cell numbers did not change so much relative to *IRX1*-overexpressed cells (Figure 7c). These findings suggested that *IRX1* gene can regulate downstream BDKRB2-PAK1 levels as well as their associated functions.

Discussion

Tumors require a blood supply for growth and hematogenous dissemination. Much attention has been focused on the role of angiogenesis, a recruitment of new vessels from pre-existing vessels. However, angiogenesis may not be the only mechanism by which tumors acquire a microcirculation. Highly aggressive tumors are capable of forming highly patterned VM that is composed of a basement membrane that stains positive with the PAS histochemical reagent in the absence of endothelial cells and fibroblasts. *IRX1* is a newly identified tumor suppressor gene. Hitherto, the tumor suppressor function of IRX1 transcription factor has been reported by us as well as by Bennett and colleagues

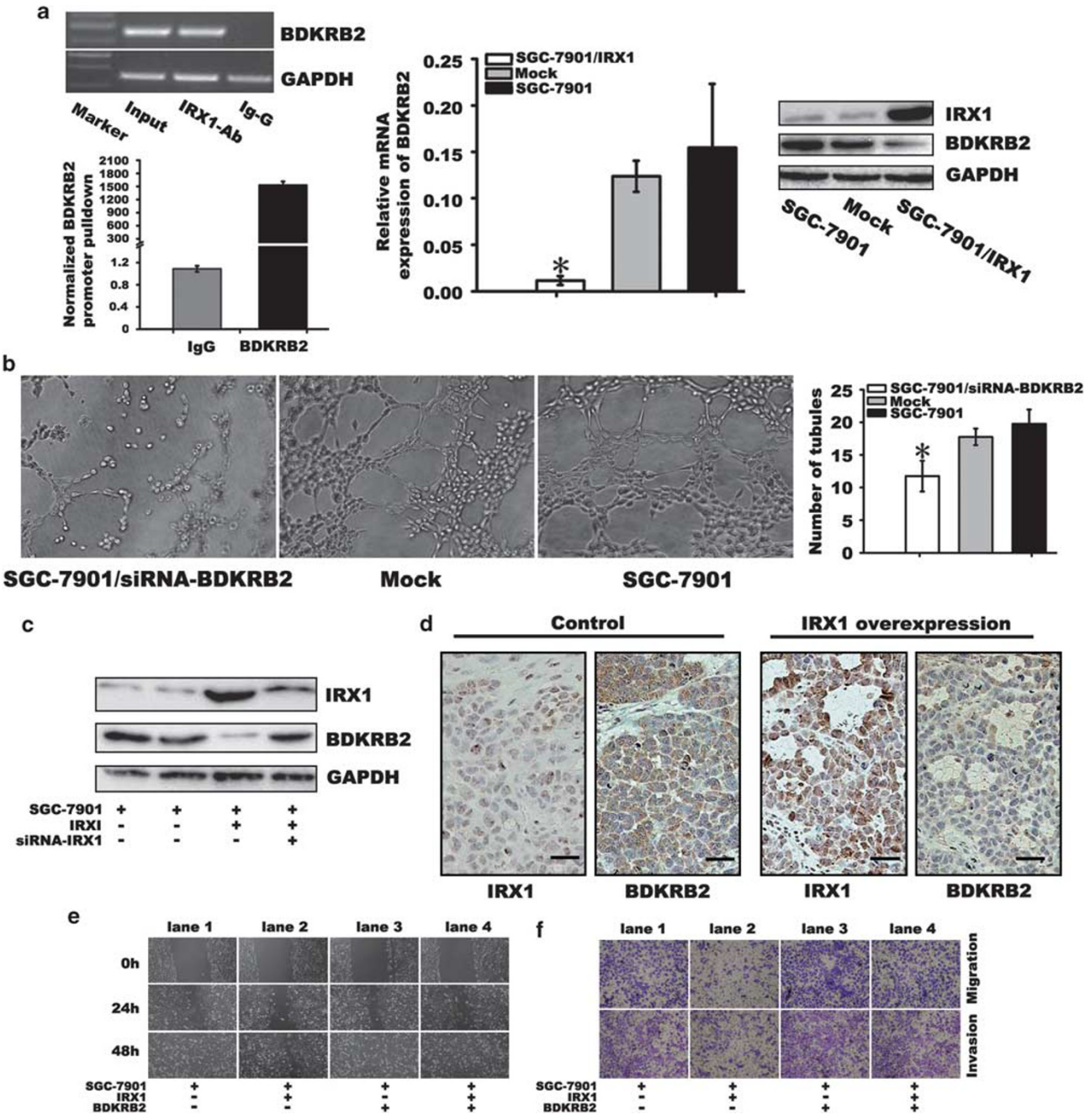

Figure 6 Analyzing the association between BDKRB2 with IRX1 and biological functions. (**a**) By chromatin immunoprecipitation, *BDKRB2*, a downstream target gene of IRX1 is identified (left). The mRNA (middle, $*P<0.001$) and protein levels (right) of BDKRB2 were significantly decreased by IRX1 overexpression. (**b**) After 48 h treatment by siRNA-*BDKRB2*, a significant reduction of endothelial tube formation was identified, compared with mock or controls by counting the tubular number (11.75 ± 2.36 vs 17.75 ± 1.25 or 19.75 ± 2.21, $*P<0.001$). The data represent the mean ± s.d. of three independent experiments. (**c**) Overexpression of IRX1 downregulated BDKRB2 expression. Whereas knocking down IRX1 by siRNA on IRX1-overexpressed cells can reverse the expressing level of BDKRB2. (**d**) Immunohistochemical staining for BDKRB2 and IRX1 on peritoneal tumor tissues of nude mice. A significant reduction of BDKRB2 expression in tumor tissue was observed at IRX1 overexpressing group, compared with control (the bar represents 20 μm). (**e**) In wound healing assay, overexpression of IRX1 alone suppressed the wound healing significantly (lane 2) and overexpression of BDKRB2 alone enhanced wound healing significantly (lane 3). Co-expression of BDKRB2 and IRX1 revealed the effect observed as control (lane 4). The mean wound distances of 7901/*IRX1*, 7901/*BDKRB2* and 7901/*IRX1*/*BDKRB2* were 322.88 ± 22.45, 53.67 ± 4.16 and 80.33 ± 3.06, respectively, at 48 h ($P<0.001$). (**f**) The similar effects on cell migration and invasion were also observed by transwell assay. The amount of migrated cells in 7901/*IRX1*, 7901/siRNA-*BDKRB2* and 7901/*IRX1*/*BDKRB2* was 31 ± 4.00 vs 165 ± 8.54 and 123 ± 3.05, respectively ($P<0.001$). The amount of invasive cells in 7901/*IRX1*, 7901/*BDKRB2* and 7901/*IRX1*/*BDKRB2* was 28.67 ± 4.04 vs 168.33 ± 3.06 and 134.33 ± 2.52, respectively ($P<0.001$). The data represent the mean ± s.d. of three independent experiments.

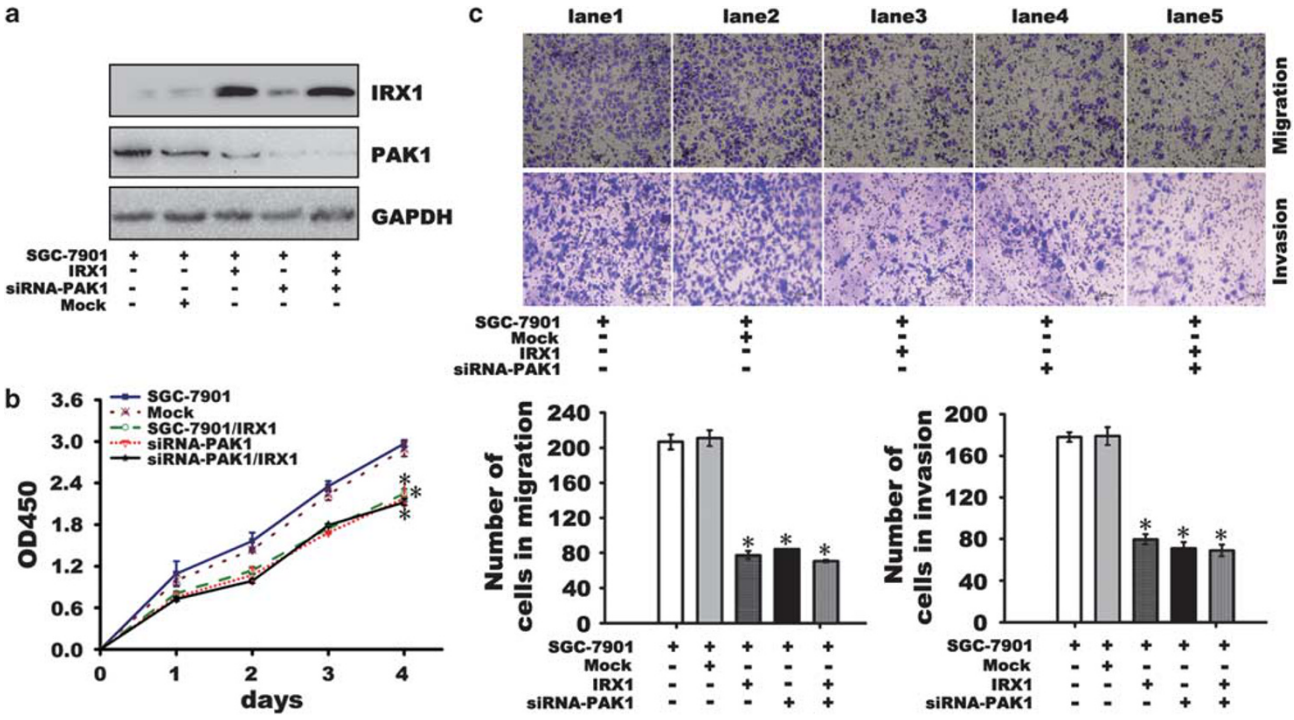

Figure 7 Observing the effect of interfering *PAK1*, an effector of BDKRB2 in *IRX1*-overexpressed cancer cells. (**a**) Overexpression of IRX1 downregulated PAK1 expressing level, whereas knockdown of PAK1 level did not alter the IRX1 level significantly. Overexpression of IRX1 combined with siRNA-PAK1 also downregulated PAK1 expressing level significantly by western blot. (**b**) The cell proliferation activity was suppressed significantly in 7901/*IRX1* or 7901/siRNA-*PAK1* groups, compared with controls ($*P<0.001$). The cell proliferation activity in 7901/*IRX1*/siRNA-*PAK1* co-transfected group was nearly the same as that observed in 7901/*IRX1* alone group ($P=0.061$). (**c**) By transwell assays, the migrated cell numbers (top) were significantly reduced in 7901/*IRX1* group (77.33 ± 4.25) or 7901/siRNA-*PAK1* group (84 ± 1), compared with control (206.66 ± 8.5, $*P<0.001$). Whereas in 7901/*IRX1*/siRNA-*PAK1* co-transfected group, the migrated cell numbers were nearly the same as that observed in 7901/*IRX1* alone group (70.66 ± 1.52 vs 77.33 ± 4.25, $P=0.202$). The invasive cell numbers (down) were significantly decreased in 7901/*IRX1* group (79.66 ± 5.03) or 7901/siRNA-*PAK1* group (71 ± 6), compared with control (178 ± 4.58, $*P<0.001$). Whereas in 7901/*IRX1*/siRNA-*PAK1* co-transfected group, the invasive cell numbers were nearly the same as that observed in 7901/siRNA-*PAK1* alone group 69 ± 5.57 vs 71 ± 6, $*P=0.113$). The data represent the mean ± s.d. of three independent experiments.

(Lu *et al*., 2005; Bennett *et al*., 2008, 2009; Guo *et al*., 2010). However, the detailed biological functions of restoring IRX1 expression on gastric cancer remain to be explored. In the present study, we further demonstrate that peritoneal spreading and long distance metastasis were arrested by restoring IRX1 expression on gastric cancer cells. These functions are mediated by interference of angiogenesis and VM formation both *in vitro* and *in vivo*. On previous microarray analysis, we found out *BDKRB2*, a downregulated gene, which involves in the regulation of blood vessels. Along with the important clue, we explored the association between IRX1 expression and angiogenesis, VM and ECM adhesive capacity.

Rich blood supply is the basis of tumor growth, spreading and metastasis. Tube formation assay is based on the ability of endothelial cells to form 3D capillary-like structures when cultured on a gel of basement membrane extract (Masamune *et al*., 2008; Nogueras *et al*., 2008). VM is a newly identified phenomenon different from traditional tumor angiogenesis. VM was first described as the fluid-conducting channels formed in highly aggressive melanoma cells by Maniotis *et al*. (1999). The channels of VM are lack of endothelial cells of liner with abundance of PAS-positive substances in the ECM. Either red blood cells or plasma could appear in those channels (Sood *et al*., 2001; Sun *et al*., 2004, 2006; van der Schaft *et al*., 2005). Importantly, one report suggested that SGC-7901 gastric cancer cells can form VM in 3D culture (Zhang, 2008). Our experiments confirmed that overexpression of IRX1 on SGC-7901 cells effectively inhibited the formation of capillary and VM structures. In chick CAM assay, another *in vivo* model for studying the angiogenic activity (Deryugina and Quigley, 2008a, b), we further confirmed that overexpression of IRX1 significantly inhibited angiogenesis on avian embryo.

Another factor that influences the process of tumor spreading and metastasis is tumor-ECM adhesive ability. During the process of metastasis, tumor cells leave the primary site, travel via blood and/or lymphatic circulatory systems, attach to the substratum of ECM at a distant site, and establish a secondary tumor, accompanied by angiogenesis of the newly formed neoplasm (Gupta and Massague, 2006; Lorch *et al*., 2007; Veeravalli *et al*., 2010). Therefore, examination of adhesive ability of tumor cells to ECM will become an important indicator for invasiveness. Our experiments

demonstrated that IRX1 overexpression weakened the adhesive ability of cell-collagen IV and cell-fibronectin adhesion.

As to blood supply of tumor, much study focused on the 'classic' genes, such as vascular endothelial growth factor (Altundag *et al*., 2004). In our studies, vascular endothelial growth factor or other metastasis-associated factor matrix metalloproteinases were not changed so much after IRX1 overexpression (Supplementary Figure 1). We found that BDKRB2 and its effector PAK1 are downregulated by IRX1 overexpression. BDKRB2 is a 9 amino acids bradykinin peptide receptor, which is constitutively expressed in vasculature. Bradykinin functions as a positive regulator for angiogenesis. BDKRB2 is overexpressed in various types of human cancer (Ishihara *et al*., 2002; Krankel *et al*., 2008). In addition, BDKRB2 interacts with integrin $\alpha5$ $\beta1$ to transactivate epidermal growth factor receptor in kidney cells (Kramarenko *et al*., 2010). Ikeda *et al*. (2004) found that antagonizing bradykinin can reduce angiogenesis and tumor growth in rats. BDKRB2 knockout mice showed decreased growth of tumor xenografts due to inhibited angiogenesis. BDKRB2 mediated induction of cyclooxygenase-2 and endothelin-1, which function as stimulators of vascular formation (Basu *et al*., 2006; Zhang *et al*., 2008; Andoh *et al*., 2010). We evaluated the roles of BDKRB2 in tumor-associated angiogenesis on cell model. RNA interference (RNAi) is a process in which double-strand RNA directs the specific degradation of a corresponding target mRNA. The mediators of this process are small double-strand RNAs, of $\sim$21 bp in length, called siRNAs (Calderon and Lavergne, 2005; Oleinikov *et al*., 2005; Bessard *et al*., 2008). siRNAs can be transfected into cells and direct the degradation of corresponding mRNAs. Hence, siRNAs represent a powerful tool for studying gene functions, as well as having the potential of being highly specific pharmaceutical agents (Gartel and Kandel, 2006; Gu *et al*., 2008). PAK, a mammalian homologs of Ser/Thr protein kinase, is the effector of bradykinin peptide receptors pathway, which has been implicated in a variety of intracellular signaling events, including cell cytoskeleton rearrangement, proliferation, cell-cycle progression, cell migration and angiogenesis (Tang *et al*., 2000; Fryer and Field, 2005; Galan Moya *et al*., 2009). Overexpression and activation of PAK has been identified in the development of cancers (Kumar and Vadlamudi, 2002; Liu *et al*., 2009). Recently, targeting PAKs have been proposed as a potential therapeutic strategy for gastric cancer (Cai *et al*., 2009; Li *et al*., 2010). In this study, protein levels of BDKRB2 and its downstream effector PAK1 were obviously downregulated by overexpression of *IRX1* gene in gastric cancer cells. We knocked down the BDKRB2 or PAK1 by RNAi and got an obvious inhibitory effect on tube formation, cell proliferation, cell migration and invasion. Our results suggested that BDKRB2 promote tumor proliferation and invasion by increased blood supply combined with other survival signals. Because BDKRB2 antagonist has been developed (Ishihara *et al*., 2002), the administration of BDKRB2 antagonist may provide a promising method for anti-cancer therapy.

In conclusion, our data, for the first time, implicate that IRX1 suppresses peritoneal spreading and long distance metastasis via inhibiting BDKRB2-dependent angiogenesis and VM mechanisms on gastric cancer. When we inhibited BDKRB2 by specific RNAi, a remarkable reduction of neovascularization was observed. BDKRB2 might be a potential target for anti-cancer strategy.

Materials and methods

Cell culture and transfection of IRX1 *gene*

Human gastric cancer cell SGC-7901 and HUVECs were preserved in our institute. Briefly, cells were grown in RPMI1640 supplemented with 10% fetal calf serum, and 2 mmol L-glutamine. Cells were maintained at 37 °C with 5% CO_2. pEGFP-N1-*IRX1* eukaryotic expression vector was constructed as previously described (Guo *et al*., 2010). pReceiver-M03-*BDKRB2* eukaryotic expression vector was purchased from FulenGen Company (Guangzhou, China). Transfectant of the empty vectors was used as controls. After 48 h incubation of SGC-7901 with transfectants, the supernatants were collected for further studies.

Endothelial tube formation assay

Angiogenesis *in vitro* was assessed by the endothelial tube formation assay kit (Cell Biolabs, San Diego, CA, USA). The tube formation assay is based on the ability of endothelial cells to form 3D capillary-like tubular structures when cultured on a gel of basement membrane extract. Briefly, each well of prechilled 96-well culture plates was coated with a thin layer of the ECM gel prepared from Engelbreth-Holm-Swarm tumor cells (50 µl/well), which was left to polymerize at 37 °C for 1 h. HUVECs were resuspended in collected supernatants from controls (SGC-7901), mock (SGC-7901/vector), SCG-7901/*IRX1*, SGC-7901/siRNA-*BDKRB2*, respectively. HUVECs (2×10^4 cells/well) were added to the polymerized ECM gel with 300 µl of the supernatants. After 18 h incubation at 37 °C with 5% CO_2, the tube formation ability was evaluated by counting the tubular number, the tubular length and tubular intersecting nods in five random fields using Image Pro Plus software (Media Cybernetics Inc., Bethesda, MD, USA; Serial No. 45N51000-33993) according to Mirshahi's method (Mirshahi *et al*., 2009). Each experiment was performed at least three times.

VM assay on 3D culture

3D type I collagen gel and matrigel mixture were produced as following: 25 µl of type I collagen (BD Bioscience, Bedford, MA, USA; 3.7 mg/ml) and matrigel (BD Bioscience) were mixed according to 1:1, dropped onto 16 mm glass cover slides in six-well culture plate. Absolute ethanol of 100 µl was added to each well until the gel was polymerized at room temperature. After a wash with PBS, 1.5×10^5 cells of SGC-7901, SGC-7901/vector and SCG-7901/*IRX1* were plated onto the gel plate. After 4-day culture without changing culture media, the cells were fixed with 4% formaldehyde in PBS for 10 min, then stained with PAS stain and counterstained with hematoxylin. The vascular mimicry formation ability was evaluated by counting the average vascular mimicry length and intersecting nods. Each experiment was performed at least three times.

Cell adhesion assay
Adhesion of tumor cells to ECM is a pivotal step in developing tumor dissemination. The CytoSelect 48-well cell adhesion kits (fibronectin-coated and collagen IV-coated; Cell Biolabs, Inc., San Diego, CA, USA) were used in this experiment. The microtiter plates were warmed up at room temperature for 10 min. The RPMI1640 was prepared according to instruction contained 0.5% bovine serum albumin, 2 mM $CaCl_2$ and 2 mM $MgCl_2$, and used to resuspend the cells of SGC-7901, SGC-7901/vector and SGC-7901/*IRX1*. A 150 μl of 1×10^6 cells/ml suspension was added to each well and incubated for 60 min. Non-specific protein binding of the coated wells was blocked by adding 1% (w/v) bovine serum albumin (4°C, 12 h) and rinsing the wells with Hepes buffer. Non-adherent cells were removed by washing three times with PBS. A 200-μl cell stain solution was added to each well and retained for 10 min at room temperature, discarding stain solution and washing three times with PBS. The total adhesive cells were determined by dissolving the attached cells in the microtiter wells with 200 μl cell extraction solution. The absorbance of each well was measured at 560 nm with microtiter plate reader (TD-20/20 analytical luminometer, Sunnyvale, CA, USA). OD showed a linear relationship to the amount of cells and was corrected for dying of bovine serum albumin/polystyrene without cells.

Chick embryo CAM assay
Fertilized chicken eggs (Xing-Huo farm, Shanghai, China) were incubated at 37 °C with humidity of 70%. On the 6th day of incubation, a round window was opened on the shell. Normally developed embryos were used for experiment. Malformated or dead embryos were excluded from experiment. The open window was sealed with transparent tape and incubated overnight. On the 7th day, a piece of sterilized filter paper disc (0.5 cm diameter) was placed on the surface of the CAM. A 30-μl collected supernatant from SGC-7901, SGC-7901/vector and SCG-7901/*IRX1* was dropped to filter paper disc daily and sealed with transparent tape for consecutive 3 days. On the 10th day of incubation, the eggs were photographed with MacroPATH dissecting microscope (Milestone, Italy). The vessel numbers around the filter paper disc were assessed. All vessels vertically to the disc or intersected with the disc at an angle greater than 45° were counted.

Nude mice study
In this experiment, both peritoneal spreading and pulmonary metastasis were observed. Four-week-old male BALB/C nude mice were purchased from the Institute of Zoology, Chinese Academy of Sciences of Shanghai. All experiments were performed in accordance with the official recommendations of the Chinese animal community. In peritoneal spreading study, 10 mice were enrolled in each group. In all, 2×10^7 cells/ml of SGC-7901, SGC-7901/vector and SCG-7901/*IRX1* were resuspended. A 0.1-ml suspension per mouse was injected intraperitoneally. In pulmonary metastasis study, 15 mice were enrolled in each group. In all, 2×10^7 cells/ml of SGC-7901, SGC-7901/vector and SCG-7901/*IRX1* were resuspended. A 0.1-ml suspension per mouse was injected into caudal vena. On the 30th day after intraperitoneal injection, mice were killed by cervical decapitation. The abdominal masses were excised and fixed with 10% buffered formalin for further morphological analysis. On the 60th day after caudal vena injection, mice were killed by cervical decapitation. The thoracic cavity of mice was examined carefully. The pulmonary metastatic masses were removed and fixed with 10% buffered formalin for further morphological analysis.

Histochemistry and immunohistochemistry
All paraffin-embedded specimens were cut into serial 5 μm sections. The sections were deparaffinized, rehydrated and subjected to histochemical and immunohistochemical staining. The immunohistochemistry was conducted with monoclonal rat anti-mouse CD34 (1:50 dilution; Abcam, Cambridge, MA, USA), mouse anti-human BDKRB2 (1:50 dilution; Abcam), rabbit anti-human IRX1 (1:50 dilution; Bioworld, Louis Park, MN, USA). Dako two-step detection Kit was used (Dako, Carpinteria, CA, USA). The histochemistry was performed with PAS staining. The slides were counterstained with hematoxylin and viewed with light microscope. Microvessel density and vascular mimicry density per mm^2 were calculated, respectively, in five random fields.

Chromatin immunoprecipitation
Chromatin immunoprecipitation assays were performed according to the kit manual (Upstate, Billerica, MA, USA). SGC-7901 cells were cultured in 1640 culture medium with 10% fetal serum, till the density of 90%, and then collected and subjected to sodium dodecyl sulfate lysation after formaldehyde crosslink of DNA and proteins at room temperature for 10 min. After sonication, antibodies of normal mouse IgG and specific antibodies to IRX1 (Abcam) were added and mixed overnight with rotation. After adding the protein G agrose to collect the antibody/antigen/DNA complex, the complex then undergo washing and elution, and reverse crosslinked by 5 M NaCl treatment in 65 °C for 5 h. Purified chromatins were then analyzed by PCR with specific primers for *BDKRB2* gene, along with control primers to detect *GAPDH* gene.

RNAi experiments
To verify the association of candidate genes with the biological functions, RNAi technology was used. SGC-7901 cells (3×10^5 cells) were plated onto six-well plates until 50% confluence. The cells were transfected with siRNA (GenePharma Co., Shanghai, China) targeting *BDKRB2*, *IRX1* and *PAK1* in accordance with the manufacturer's instructions (the sequences of siRNAs were listed in Supplementary Table). Briefly, a 10-μl transfection reagent was incubated with 500 μl OPTI-MEM medium (Gibco, Carlsbad, CA, USA) for 5 min. Subsequently, siRNAs were added to wells (120 nmol/l). After 2 days transfection, cells were collected for protein expressing analysis.

Invasion, migration and cell viability assays
Cell invasion and cell migration assay were performed. The transwell chamber was used (8 μm, 24-well format; Corning, Lowell, MA, USA). In invasion assay, the insert membranes were coated with diluted Matrigel (BD Biosciences). Cells (1×10^5) were added to upper chamber and cultured for 48 h. In migration assay, the insert membranes were not coated with Matrigel and cultured in the same condition. Finally, the insert membranes were cut and stained with Crystal violet (0.04% in water; 100 μl) and counted the permeating cells under the inverted microscope and photographed. Meanwhile, the cell viability (1×10^5) of different groups with same culture conditions was also assayed at 0, 24 and 48 h time points by cell counter (Coulter, Sequim, WA, USA). At least three independent experiments were performed for all conditions. The data are shown as means ± s.d.

Protein analysis
Protein lysates were prepared from collected cells in lysis buffer containing 20 mM/l Hepes, 0.15 M NaCl and 1% Triton X-100 supplemented with 80 μl/ml phosphatase inhibitor cocktail II (Sigma, St Louis, MO, USA) and 10 μl/ml

complete protease inhibitor cocktail (Boehringer Mannheim GmbH, Indianapolis, IN, USA). Protein was quantified by Bio-Rad protein assay kit (Bio-Rad, Hercules, CA, USA), with bovine serum albumin as control. Protein (100 μg) was separated by 8% sodium dodecyl sulfate polyacrylamide gel electrophoresis. Membrane was detected by BDKRB2, IRX1 and PAK1 antibodies. GAPDH antibody was used for internal control (Supplementary Table).

Statistics

Data are shown as mean ± s.d. The statistical difference between the two groups was examined by Student's *t*-test. Multiple comparisons were performed by one-way analysis of variance. $P < 0.05$ was considered statistically significant.

Conflict of interest

The authors declare no conflict of interest.

Acknowledgements

This work was supported, in part, by grants from the National Natural Science Foundation of China (30572127, 30770961 and 30973486), the Chinese National High Tech Program (863-2006AA02A402 and 2006AA02A301), Key Research Project from Shanghai Science and Technology Commission (09DZ1950101 and 09JC1409600) and Shanghai Charity Foundation for Cancer Research.

References

Alarcon P, Rodriguez-Seguel E, Fernandez-Gonzalez A, Rubio R, Gomez-Skarmeta JL. (2008). A dual requirement for Iroquois genes during Xenopus kidney development. *Development* **135**: 3197–3207.

Altundag K, Elkiran ET, Altundag O. (2004). Vascular endothelial growth factor is associated with the efficacy of endocrine therapy in patients with advanced breast carcinoma. *Cancer* **100**: 1768–1769; author reply 1769.

Andoh T, Akira A, Saiki I, Kuraishi Y. (2010). Bradykinin increases the secretion and expression of endothelin-1 through kinin B2 receptors in melanoma cells. *Peptides* **31**: 238–241.

Basu GD, Liang WS, Stephan DA, Wegener LT, Conley CR, Pockaj BA *et al*. (2006). A novel role for cyclooxygenase-2 in regulating vascular channel formation by human breast cancer cells. *Breast Cancer Res* **8**: R69.

Becker MB, Zulch A, Bosse A, Gruss P. (2001). Irx1 and Irx2 expression in early lung development. *Mech Dev* **106**: 155–158.

Bennett KL, Karpenko M, Lin MT, Claus R, Arab K, Dyckhoff G *et al*. (2008). Frequently methylated tumor suppressor genes in head and neck squamous cell carcinoma. *Cancer Res* **68**: 4494–4499.

Bennett KL, Romigh T, Eng C. (2009). Disruption of transforming growth factor-beta signaling by five frequently methylated genes leads to head and neck squamous cell carcinoma pathogenesis. *Cancer Res* **69**: 9301–9305.

Bessard A, Fremin C, Ezan F, Fautrel A, Gailhouste L, Baffet G. (2008). RNAi-mediated ERK2 knockdown inhibits growth of tumor cells *in vitro* and *in vivo*. *Oncogene* **27**: 5315–5325.

Cai XZ, Wang J, Li XD, Wang GL, Liu FN, Cheng MS *et al*. (2009). Curcumin suppresses proliferation and invasion in human gastric cancer cells by downregulation of PAK1 activity and cyclin D1 expression. *Cancer Biol Ther* **8**: 1360–1368.

Calderon AJ, Lavergne JA. (2005). RNA interference: a novel and physiologic mechanism of gene silencing with great therapeutic potential. *PR Health Sci J* **24**: 27–33.

Deryugina EI, Quigley JP. (2008a). Chapter 2 Chick embryo chorioallantoic membrane models to quantify angiogenesis induced by inflammatory and tumor cells or purified effector molecules. *Methods Enzymol* **444**: 21–41.

Deryugina EI, Quigley JP. (2008b). Chick embryo chorioallantoic membrane model systems to study and visualize human tumor cell metastasis. *Histochem Cell Biol* **130**: 1119–1130.

Fryer BH, Field J. (2005). Rho, Rac, Pak and angiogenesis: old roles and newly identified responsibilities in endothelial cells. *Cancer Lett* **229**: 13–23.

Fujimoto A, Onodera H, Mori A, Nagayama S, Yonenaga Y, Tachibana T. (2006). Tumour plasticity and extravascular circulation in ECV304 human bladder carcinoma cells. *Anticancer Res* **26**: 59–69.

Galan Moya EM, Le Guelte A, Gavard J. (2009). PAKing up to the endothelium. *Cell Signal* **21**: 1727–1737.

Gartel AL, Kandel ES. (2006). RNA interference in cancer. *Biomol Eng* **23**: 17–34.

Getmanova EV, Chen Y, Bloom L, Gokemeijer J, Shamah S, Warikoo V *et al*. (2006). Antagonists to human and mouse vascular endothelial growth factor receptor 2 generated by directed protein evolution *in vitro*. *Chem Biol* **13**: 549–556.

Gu W, Putral L, McMillan N. (2008). siRNA and shRNA as anticancer agents in a cervical cancer model. *Methods Mol Biol* **442**: 159–172.

Guo X, Liu W, Pan Y, Ni P, Ji J, Guo L *et al*. (2010). Homeobox gene IRX1 is a tumor suppressor gene in gastric carcinoma. *Oncogene* **29**: 3908–3920.

Gupta GP, Massague J. (2006). Cancer metastasis: building a framework. *Cell* **127**: 679–695.

Hao X, Sun B, Zhang S, Zhao X. (2002). Microarray study of vasculogenic mimicry in bi-directional differentiation malignant tumor. *Zhonghua Yi Xue Za Zhi* **82**: 1298–1302.

Ikeda Y, Hayashi I, Kamoshita E, Yamazaki A, Endo H, Ishihara K *et al*. (2004). Host stromal bradykinin B2 receptor signaling facilitates tumor-associated angiogenesis and tumor growth. *Cancer Res* **64**: 5178–5185.

Ishihara K, Kamata M, Hayashi I, Yamashina S, Majima M. (2002). Roles of bradykinin in vascular permeability and angiogenesis in solid tumor. *Int Immunopharmacol* **2**: 499–509.

Kramarenko II, Bunni MA, Raymond JR, Garnovskaya MN. (2010). Bradykinin B2 receptor interacts with integrin alpha5beta1 to transactivate epidermal growth factor receptor in kidney cells. *Mol Pharmacol* **78**: 126–134.

Krankel N, Katare RG, Siragusa M, Barcelos LS, Campagnolo P, Mangialardi G *et al*. (2008). Role of kinin B2 receptor signaling in the recruitment of circulating progenitor cells with neovascularization potential. *Circ Res* **103**: 1335–1343.

Kumar R, Vadlamudi RK. (2002). Emerging functions of p21-activated kinases in human cancer cells. *J Cell Physiol* **193**: 133–144.

Li X, Liu F, Li F. (2010). PAK as a therapeutic target in gastric cancer. *Expert Opin Ther Targets* **14**: 419–433.

Liu F, Li X, Wang C, Cai X, Du Z, Xu H *et al*. (2009). Downregulation of p21-activated kinase-1 inhibits the growth of gastric cancer cells involving cyclin B1. *Int J Cancer* **125**: 2511–2519.

Lorch JH, Thomas TO, Schmoll HJ. (2007). Bortezomib inhibits cell-cell adhesion and cell migration and enhances epidermal growth factor receptor inhibitor-induced cell death in squamous cell cancer. *Cancer Res* **67**: 727–734.

Lu Y, Yu Y, Zhu Z, Xu H, Ji J, Bu L *et al*. (2005). Identification of a new target region by loss of heterozygosity at 5p15.33 in sporadic gastric carcinomas: genotype and phenotype related. *Cancer Lett* **224**: 329–337.

Maniotis AJ, Folberg R, Hess A, Seftor EA, Gardner LM, Pe'er J *et al*. (1999). Vascular channel formation by human melanoma cells *in vivo* and *in vitro*: vasculogenic mimicry. *Am J Pathol* **155**: 739–752.

Masamune A, Kikuta K, Watanabe T, Satoh K, Hirota M, Shimosegawa T. (2008). Hypoxia stimulates pancreatic stellate cells to induce fibrosis and angiogenesis in pancreatic cancer. *Am J Physiol Gastrointest Liver Physiol* **295**: G709–G717.

Matsuda KM, Madoiwa S, Hasumi Y, Kanazawa T, Saga Y, Kume A *et al*. (2000). A novel strategy for the tumor angiogenesis-targeted gene therapy: generation of angiostatin from endogenous plasminogen by protease gene transfer. *Cancer Gene Ther* **7**: 589–596.

Mirshahi P, Rafii A, Vincent L, Berthaut A, Varin R, Kalantar G *et al*. (2009). Vasculogenic mimicry of acute leukemic bone marrow stromal cells. *Leukemia* **23**: 1039–1048.

Nogueras S, Merino A, Ojeda R, Carracedo J, Rodriguez M, Martin-Malo A *et al*. (2008). Coupling of endothelial injury and repair: an analysis using an *in vivo* experimental model. *Am J Physiol Heart Circ Physiol* **294**: H708–H713.

Oleinikov AV, Zhao J, Gray MD. (2005). RNA interference by mixtures of siRNAs prepared using custom oligonucleotide arrays. *Nucleic Acids Res* **33**: e92.

Sharma N, Seftor RE, Seftor EA, Gruman LM, Heidger Jr PM, Cohen MB *et al*. (2002). Prostatic tumor cell plasticity involves cooperative interactions of distinct phenotypic subpopulations: role in vasculogenic mimicry. *Prostate* **50**: 189–201.

Shirakawa K, Kobayashi H, Sobajima J, Hashimoto D, Shimizu A, Wakasugi H. (2003). Inflammatory breast cancer: vasculogenic mimicry and its hemodynamics of an inflammatory breast cancer xenograft model. *Breast Cancer Res* **5**: 136–139.

Sood AK, Seftor EA, Fletcher MS, Gardner LM, Heidger PM, Buller RE *et al*. (2001). Molecular determinants of ovarian cancer plasticity. *Am J Pathol* **158**: 1279–1288.

Su M, Feng YJ, Yao LQ, Cheng MJ, Xu CJ, Huang Y *et al*. (2008). Plasticity of ovarian cancer cell SKOV3ip and vasculogenic mimicry *in vivo*. *Int J Gynecol Cancer* **18**: 476–486.

Sun B, Qie S, Zhang S, Sun T, Zhao X, Gao S *et al*. (2008). Role and mechanism of vasculogenic mimicry in gastrointestinal stromal tumors. *Hum Pathol* **39**: 444–451.

Sun B, Zhang S, Zhang D, Du J, Guo H, Zhao X *et al*. (2006). Vasculogenic mimicry is associated with high tumor grade, invasion and metastasis, and short survival in patients with hepatocellular carcinoma. *Oncol Rep* **16**: 693–698.

Sun B, Zhang S, Zhao X, Zhang W, Hao X. (2004). Vasculogenic mimicry is associated with poor survival in patients with mesothelial sarcomas and alveolar rhabdomyosarcomas. *Int J Oncol* **25**: 1609–1614.

Tang Y, Zhou H, Chen A, Pittman RN, Field J. (2000). The Akt proto-oncogene links Ras to Pak and cell survival signals. *J Biol Chem* **275**: 9106–9109.

van der Schaft DW, Hillen F, Pauwels P, Kirschmann DA, Castermans K, Egbrink MG *et al*. (2005). Tumor cell plasticity in Ewing sarcoma, an alternative circulatory system stimulated by hypoxia. *Cancer Res* **65**: 11520–11528.

Veeravalli KK, Chetty C, Ponnala S, Gondi CS, Lakka SS, Fassett D *et al*. (2010). MMP-9, uPAR and cathepsin B silencing downregulate integrins in human glioma xenograft cells *in vitro* and *in vivo* in nude mice. *PLoS One* **5**: e11583.

Wu J, Akaike T, Hayashida K, Miyamoto Y, Nakagawa T, Miyakawa K *et al*. (2002). Identification of bradykinin receptors in clinical cancer specimens and murine tumor tissues. *Int J Cancer* **98**: 29–35.

Yue WY, Chen ZP. (2005). Does vasculogenic mimicry exist in astrocytoma? *J Histochem Cytochem* **53**: 997–1002.

Zhang J. (2008). Morphology and mechanism research of gastric cancer vasculogenic mimicry. *J Chongqing Medical University* **33**: 1603–1605.

Zhang S, Zhang D, Sun B. (2007). Vasculogenic mimicry: current status and future prospects. *Cancer Lett* **254**: 157–164.

Zhang W, Bhola N, Kalyankrishna S, Gooding W, Hunt J, Seethala R *et al*. (2008). Kinin b2 receptor mediates induction of cyclooxygenase-2 and is overexpressed in head and neck squamous cell carcinomas. *Mol Cancer Res* **6**: 1946–1956.

Supplementary Information accompanies the paper on the Oncogene website (http://www.nature.com/onc)